JOURNAL OF MATERIALS SCIENCE 1 (1966) 29–40

Differential Thermal Analysis and X-ray Diffraction Study of Devitrification Processes

Part 1 Li_2O-B_2O_3-SiO_2 Glasses

L. F. OLDFIELD, D. J. HARWOOD, B. LEWIS
The General Electric Co Ltd, Central Research Laboratories, Hirst Research Centre, Wembley, UK

Received 22 October 1965

Glasses of compositions lying in the immediate neighbourhood of the tie-line between $Li_2O.\ 2SiO_2$ and $Li_2O.\ 2B_2O_3$ have been investigated by DTA. The endotherm peak temperatures were shown to be in general agreement with the eutectic and liquidus values proposed by Sastry and Hummel.

These glasses were devitrified by heat treatment at the exotherm peak temperatures and the crystalline products were determined by X-ray diffraction analysis. Certain compositions near to the eutectic, and within the two-liquid field, devitrified to give three or four crystalline phases. The resultant material in each case was hard and non-porous and of potential use as a glass-ceramic. Compositions in the lithium diborate field also devitrified to give well-sintered products.

1. Introduction

Glass-ceramics are polycrystalline solids prepared by the controlled crystallisation of glasses [1]. Devitrification is achieved by subjecting a suitable homogeneous glass to a predetermined heat treatment schedule so that nucleation and subsequent growth of the crystals occur in a satisfactory manner. Preferably, the resultant product should contain sub-micron crystals with only a small proportion of residual glassy phase. Uniform crystallisation can be achieved by the deliberate addition of nucleation catalysts, such as a very dilute dispersion of a noble metal, in the glass. Another method uses a glass composition, which is homogeneous at high temperatures but separates into two vitreous phases at moderate temperatures, one phase consisting of sub-micron droplets uniformly dispersed within the second phase. Such droplets can assume the form of nearly perfect spheres or lenses.

Lithium borosilicate glasses show phase separations of this liquid-in-liquid type and these are easily detectable by electron microscopy even in some cases of quenched specimens [2]. Such glasses may therefore form the basis for the development of glass-ceramics. The present investigation was limited to compositions in the immediate neighbourhood of the $Li_2O.\ 2SiO_2$ field, particularly the tie-line between this compound and $Li_2O.\ 2B_2O_3$ and also the near-by regions of the two-liquid field. The phase equilibrium relations have been reported by Sastry and Hummel [3] and those relevant to the present case are shown in fig. 1.

2. DTA of Glass-Ceramics

The heat treatment required to convert glass into ceramic is normally carried out between the annealing temperature of the primary glass and the lowest eutectic or melting point of the crystalline phase(s) in the devitrified material. Differential thermal analysis (DTA) can be used to determine the annealing temperature and the various eutectics, liquidi or melting points in the glass/glass-ceramic system. These appear as endotherms on the DTA trace [4, 5]. Devitrification

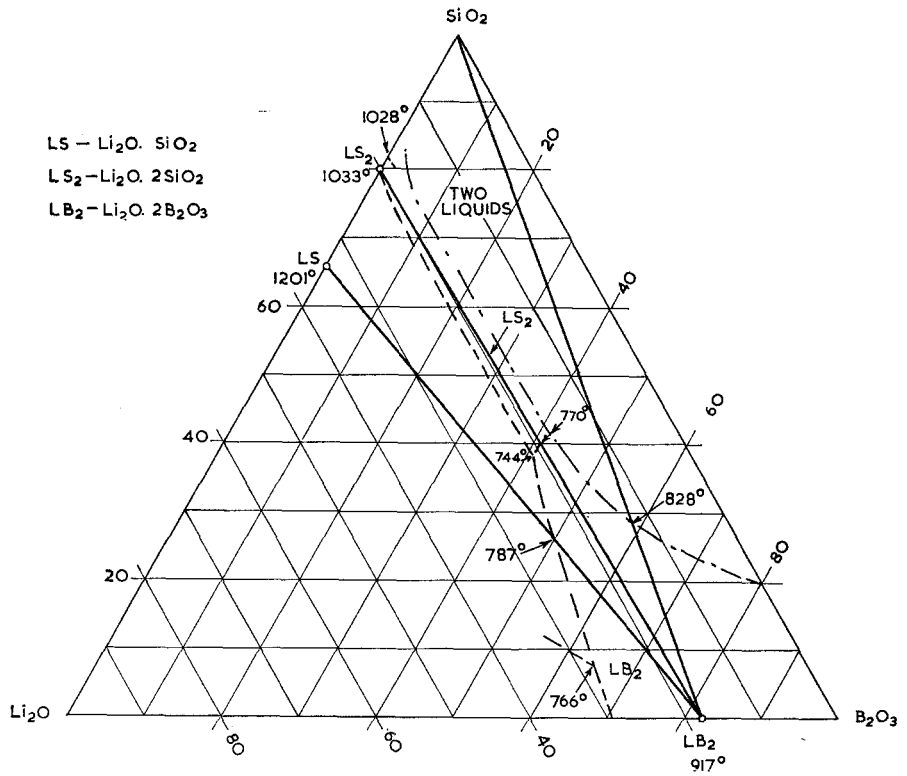

Figure 1 Some phase relations in the lithium borosilicate system, after Sastry and Hummel [3]. LS—$Li_2O.SiO_2$; LS_2—$Li_2O.2SiO_2$; LB_2—$Li_2O.2B_2O_3$.

is exothermic and the DTA exotherm peak temperatures can be used to characterise the glass-ceramic conversion process [5]. Russell and Bergeron [6] showed that the DTA exotherm for crystal growth may occur as much as 100 to 150° C below the temperature of the maximum rate of crystal growth. The peak corresponded to a temperature at which surface nucleation was relatively high and the growth rate was low. Thakur *et al* [5] showed that a nucleation catalyst, platinum, also lowered the exotherm peak temperature by 10 to 30° C.

However, the main objective in heat treatment is to achieve many nuclei growing to small crystals and not the maximum size of crystals. A good compromise is obtained, especially with fine glass powders, by treatments at, or near, the main DTA exotherms. This knowledge of the DTA exotherms is especially useful for devitrifying: (i) pressed compacts of glass powders to pre-form glass-ceramic components to be used in sealing to glass, metal or a ceramic; or (ii) slurries used for painting surfaces to be sealed subsequently (solder glass-ceramics). In many cases, these sealing glass compositions are not nucleated deliberately and the devitrification proceeds from the surfaces of the fine particles.

3. Experimental

3.1. Glass Compositions

These are given in tables I and II and figs. 2 and 3.

Analar lithium carbonate, boric oxide glass (Borax Consolidated Ltd) and crushed Brazilian rock crystal were used for batch materials. The glasses were melted in Pt/2% Rh alloy crucibles in an electric furnace heated by silicon carbide elements. Melting temperatures were in the range 1200 to 1450° C for times between 30 min and 24 h. No allowance was made for volatilisation losses. After melting, the glasses were dragaded*, dried and ball-milled. The powder was then sieved to an upper size limit of 150 mesh/in^2. This material gave uniform devitrification during the DTA heat treatment.

*Dragading is the rapid quenching of a thin stream of molten glass in a very large volume of cold water.

TABLE I Compositions of lithium borosilicate glasses. Heat treatments and X-ray diffraction analyses of the sintered products. Silica-rich series

Sample	Wt % Glass composition B_2O_3	Li_2O	SiO_2	Temperature of main exothermic peak °C	Peak* strength μV	Temperature of heat treatment† °C	Time h	Degree of sintering	Crystalline phases in sintered product in order of concentration (from X-ray analysis)
C1	—	20	80	540	450	530	½	0	Lithium disilicate + ~10% lithium metasilicate, $Li_2O.SiO_2$
C2	5	19	76	554	260	550	½	1	—
C3	10	18	72	563	290	550	½	1	Lithium disilicate + ~5% lithium metasilicate.
C4	15	17	68	582	170	570	1	2	—
C5	20	16	64	598	120	590	2	2	Lithium disilicate + 10 − 15% unidentified material.
C6	30	14	56	615	100	610	3	3	Lithium disilicate + lithium diborate (< 40%) + 5 to 10% unidentified material.
C11	—	15.0	85.0	588	90	570	2	0	Lithium disilicate + 5% lithium metasilicate.
C12	5.0	14.2	80.8	579	120	570	2	0	Lithium disilicate single phase.
C13	10.0	13.5	76.5	580	130	570	2	0	—
C14	15.0	12.7	72.3	622	60	610	3	1	Lithium disilicate + α-quartz + unidentified material (possible containing $Li_2O.2B_2O_3$).
C15	20.0	12.0	68.0	651	40	650	4	2	—
C16	30.0	10.5	59.5	667	20	650	4	3	α-quartz + lithium diborate + lithium disilicate.
C21	—	25.0	75.0	532	410	530	½	0	Lithium metasilicate + 10 − 20% lithium disilicate.
C22	5.0	23.7	71.3	537	310	530	½	0	—
C23	10.0	22.5	67.5	560	320	550	½	0	Lithium disilicate + lithium metasilicate in approximately equal amounts.
C24	15.0	21.2	63.8	579	180	570	1	0-1	—
C25	20.0	20.0	60.0	607	130	590	2	2	Lithium disilicate + lithium metasilicate in approximately equal amounts.
C26	30.0	17.5	52.5	634	80	630	3	3	Lithium disilicate + lithium diborate (< 40%) − 5 to 10% unidentified material.
Cα	—	20.0	80.0	548	440	530	½	0	
Cβ	5.0	19.8	75.2	563	350	550	½	0	Lithium disilicate + ~5% lithium metasilicate.
Cγ	10.0	19.6	70.4	566	300	550	½	1	—
Cδ	15.0	19.4	65.6	581	180	570	1	2	Lithium disilicate + 10 to 20% lithium metasilicate.
Cε	20.0	19.2	60.8	604	130	590	2	2	—
Cζ	25.0	19.0	56.0	629	70	610	3	3	Lithium metasilicate + lithium disilicate + α-quartz + unidentified material.
Cη	30.0	18.8	51.2	644	70	630	3	3	—
Cθ	35.0	18.6	46.4	636	50	630	3	3	Lithium disilicate + lithium diborate. (~40%) + 5 to 10% unidentified material.

*Peak strength = height of peak in μV.

†Heat treatment temperatures at nearest 20° C below the peak temperature to reduce the number of separate treatments.

TABLE II Compositions of lithium borosilicate glasses. Heat treatments and X-ray diffraction analyses of the sintered products. Boric oxide-rich series

Sample	Wt % Glass composition B_2O_3	Li_2O	SiO_2	Temperature of main exothermic peak °C	Peak* strength μV	Temperature of heat treatment† °C	Time h	Degree of sintering	Crystalline phases in sintered product in order of concentration (from X-ray analysis)
D00	40	20	40	610	40	—	—	—	—
D0	45	20	35	620,715	60,60	—	—	—	—
D1	50	20	30	680	190	680	1	3	Lithium diborate, lithium metasilicate, lithium disilicate + α-quartz.
D2	55	20	25	590	200	590	1	3	Lithium diborate, lithium metasilicate + unidentified phase.
D3	60	20	20	615	440	590	½	3	Phase constitution as for D2.
D4	65	20	15	680	230	680	1	3	Phase constitution as for D1.
D5	70	20	10	560	320	560	½	3	Phase constitution as for D2 but the three phases are now present in approximately equal proportions.
D6	75	20	5	530	370	530	½	3	Essentially lithium diborate + small amount of lithium metasilicate and unidentified material.
D11	55	15	30	655	310	650	⅔	3	Lithium diborate major phase.
D12	60	15	25	545	480	530	½	3	Minor phases of lithium disilicate and α-quartz decrease in the series D11 → D13
D13	65	15	20	590	410	590	½	3	
D14	70	15	15	620	520	620	⅓	3	Essentially lithium diborate + small amount of α-quartz.
D15	75	15	10	570	340	560	½	3	Lithium diborate
D16	80	15	5	585	500	590	½	3	Lithium diborate + small amount of unidentified material.

*Peak strength = height of peak in μV.
†Heat treatment temperatures at nearest 20° C below the peak temperature to reduce the number of separate treatments.

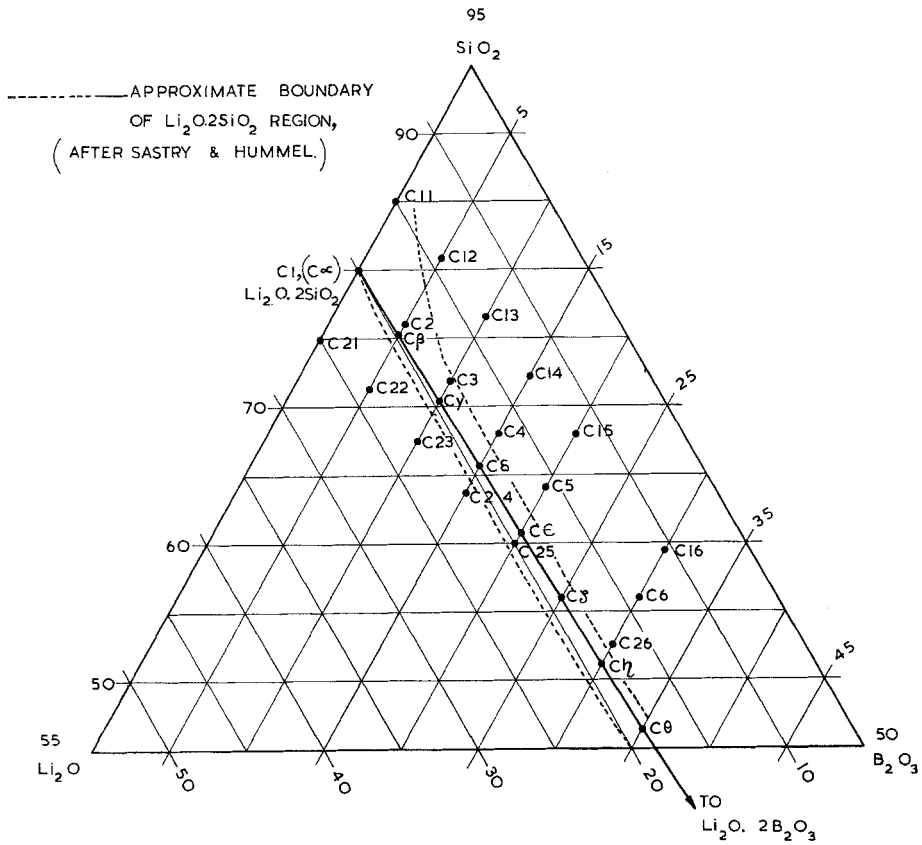

Figure 2 Lithium borosilicate system, silica-rich C series compositions.

3.2. Sintered and Devitrified Products for X-ray Analysis

Glass powder passing 150 mesh/in^2 was suspended in a binder consisting of 3% nitrocellulose in butyl acetate to form a thick paste. This was then heated in air in a heat-resistant metal tray in an electric muffle with heating and cooling rates of 3 to 5° C/min. Heat treatments were carried out at temperatures in the region of the main DTA exothermic peak determined for each composition, for times inversely proportional to the peak height or strength (see tables I and II). Satisfactorily devitrified products suitable for X-ray analysis were obtained using the scale of 2 h corresponding to a peak "height" of 100 μV measured by the differential Pt/13% Rh/Pt thermocouple; 100μV corresponds to a difference of 8 to 9° C in the range 500 to 700° C.

This scale was chosen arbitrarily to cover a wide range of devitrifying glasses of very different compositions. The maximum allowable time in processing was 4 h heat treatment. Compositions giving small exotherm peaks ($\leqslant$ 4 to 5° C, corresponding to $\leqslant$ 50μV) were thus subjected to 4 h heat treatment, compositions with larger peaks, 5 to 10° C, were given 3 h treatment, and so on. It was also considered that prolonged heat treatment would produce secondary phases in sufficient quantity for X-ray identification. Subsequent tests showed that the major phase crystallised within a short time at the holding temperature, $\sim$ 10 to 20 mins, and was then present in its maximum concentration and crystallite size. The secondary phases developed more slowly and their proportion tended to increase with the period of heat treatment. As the concentration of the major phase was unchanged it is presumed that the minor phases resulted from devitrification of the residual glassy phase.

The heat-treated products were graded according to the degree of sintering achieved, as follows:

Grade 0 – unsintered, still in powder form.

Grade 1 – slightly sintered, easily crumbled between the fingers.

Grade 2 – sintered to a fairly hard mass, but

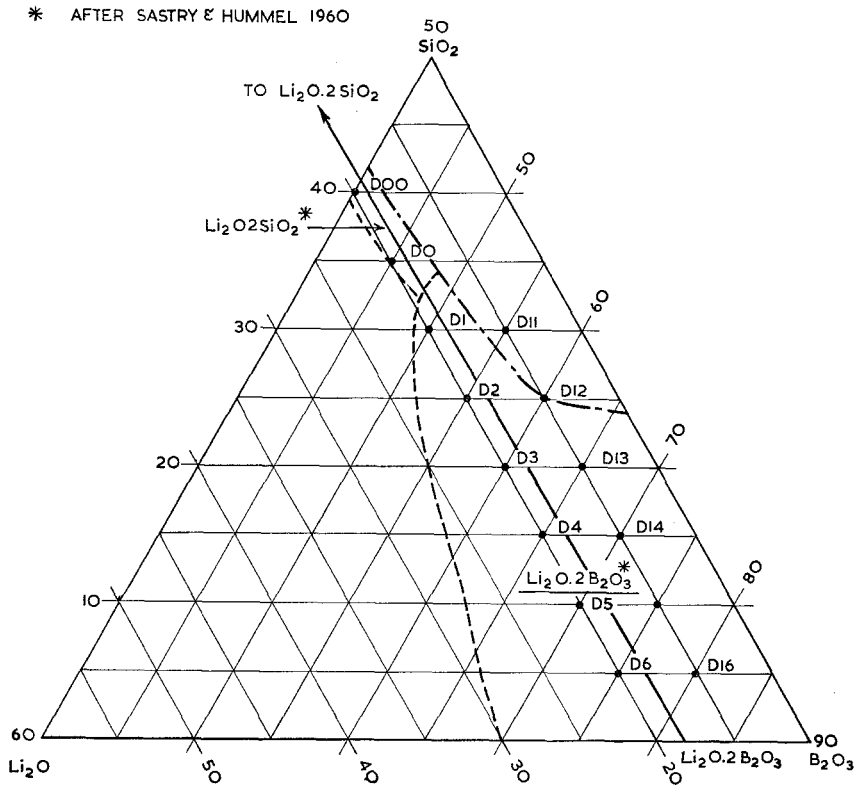

Figure 3 Lithium borosilicate system. Boric oxide-rich D series compositions lying along the $Li_2O.2SiO_2$—$Li_2O.2B_2O_3$ join.

very porous and easily powdered by scratching with a steel tool.

Grade 3 – well sintered to a hard, dense mass requiring a diamond wheel to cut it. This material could be used as a glass-ceramic.

3.3. Apparatus for DTA Measurements

The furnace and crucible system were designed originally for the investigation of glass batch reactions [7]. The vertical cylindrical furnace was wound to give a uniform hot zone in the region of the crucible-thermocouple assembly (fig. 4). A sand seal, refractory column, and large refractory furnace stopper, together with a refractory crucible shield, effectively reduced convective effects.

A pulley and counterweight system enabled the furnace to be lifted vertically clear of the crucible assembly when changes in samples were required. This system, together with circular grooves in the pyrophyllite to accommodate the crucible skirts, was designed to ensure reproducible positioning of the furnace and crucible assembly.

The crucibles of Pt/2% Rh alloy were indented to take the junctions of Pt/Pt/13% Rh thermocouples using 0.25 mm diameter wire. The crucibles were designed specifically to allow for the volume changes which occur during batch reactions and sintering. The sample temperature and the differential temperature emf's were measured by a Leeds and Northrup $X_1 - X_2$ recorder, the output from the differential thermocouple being preamplified by a Leeds and Northrup 9835 B d.c. amplifier.

Analar grade alumina powder was used as reference material in all cases. Samples of 2g of powdered glasses were used for each DTA run and a linear rate of increasing temperature of 10° C/min was used.

4. Results

4.1. Silica-Rich Compositions

4.1.1. DTA Results

DTA curves are given in fig. 5 for the compositions lying on the $Li_2O.2SiO_2 - Li_2O.2B_2O_3$ join from pure $Li_2O.2SiO_2$ to approximately 50% $Li_2O.2B_2O_3$. The "annealing dip" became more pronounced as the B_2O_3 content increased and moved to slightly higher temperatures from

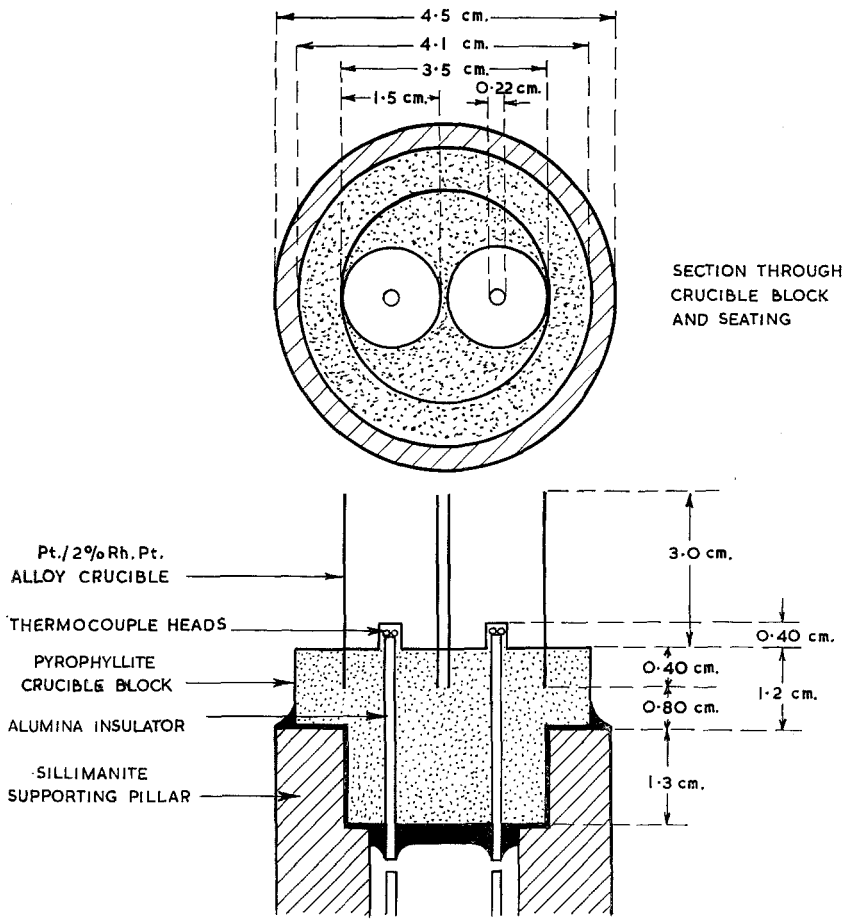

Figure 4 Crucibles and crucible assembly.

500 to 550° C. The exothermic peak became less pronounced with increasing B_2O_3 content and moved to higher temperatures. The endothermic peak also became less pronounced with increasing B_2O_3, but moved to lower temperatures.

Peak temperatures, excluding "annealing dips", are plotted against B_2O_3 content in fig. 6a and b. The endothermic peaks correspond to the liquidi of the compositions resulting from the DTA temperature programme and are generally 30 to 40° C lower than those found by Sastry and Hummel [3] from equilibrium studies, although there is good agreement for $Li_2O.2SiO_2$ (mp 1037° compared with 1033° C) (fig. 6a). The lower DTA liquidus values may be due to the presence of a higher proportion of liquid glassy phase as compared with the equilibrated material.

Three-dimensional diagrams are given in figs. 7a, b and c for all the compositions investigated in this part of the system. These show the temperature and height of the main exothermic peak and the temperature of the endothermic peak respectively.

Fig. 7a shows that the exothermic peak temperature increased markedly with increasing B_2O_3 content and slightly with decreasing Li_2O content. Fig. 7b shows that the height of the exothermic peak increased with increasing SiO_2 and Li_2O contents. Fig. 7c shows that the endothermic peak temperature decreased markedly with increasing B_2O_3 content.

It may be concluded from these results that B_2O_3 acts as a diluent in the devitrification process during the DTA run, and that the temperature-composition relationships are consistent with the phase equilibrium diagram although not in exact agreement with them. The height of the exothermic peak is approximately proportional to the degree of devitrification

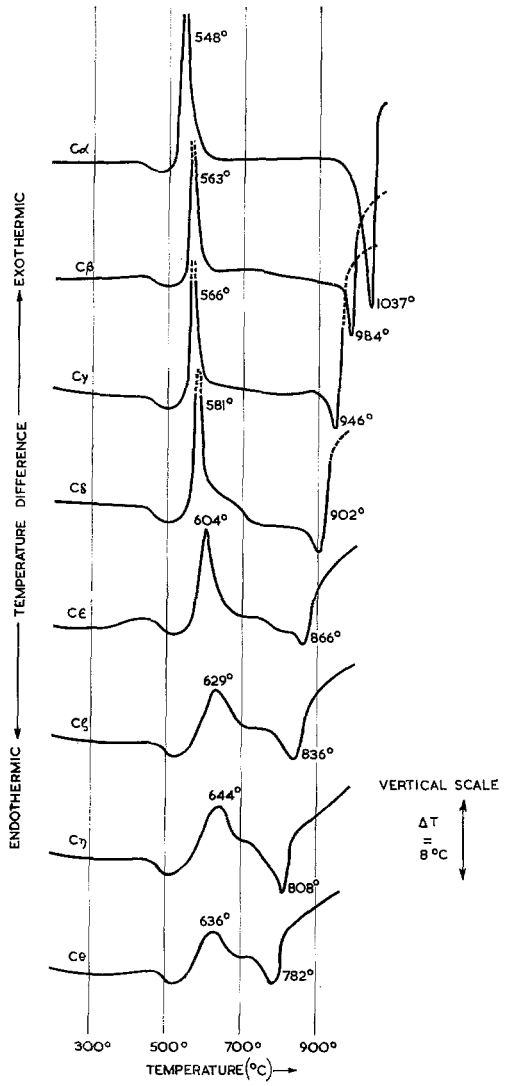

Figure 5 Differential thermal analysis of lithium borosilicate system. Silica-rich compositions lying along the $Li_2O.2SiO_2$-$Li_2O.2B_2O_3$ join.

achieved. A more accurate assessment of this is given by the area under the peak. This is proportional to the total heat evolved in the devitrification process [8]. This statement strictly applies only when one crystalline phase is precipitated; unless each phase has the same heat of crystallisation. The crystallographic analyses discussed below indicate that co-crystallisation does occur in most cases.

The areas under the main exothermic peaks are given in arbitrary units in table III for comparison. The reproducibility is good for a given composition. In general, the areas decrease with increasing B_2O_3 content; the most obvious trend being shown by the Cα series.

4.1.2. X-ray Analysis of Sintered Products

Sintered products were prepared in the manner described above and the relevant data are given in table I. All heat treatments were carried out well below 770° C, the eutectic of the system. The compositions highest in SiO_2 did not sinter, i.e. there was no cohesion between the particles which were entirely crystalline. The compositions highest in B_2O_3 gave dense, sintered bodies similar to glass-ceramics in texture.

The chief crystalline phase formed in samples containing no, or only small amounts of, B_2O_3 has been identified as lithium disilicate. This phase is the polymorphic form of lithium disilicate reported by Rindone [9] to be stable below 936° C.

The addition of B_2O_3 in relatively low concentrations did not alter the identity of the first phase to crystallise, but increased the proportion of the sample which was retained in the vitreous form. When further increases in B_2O_3 content were made, several phases crystallised together. For example, α-quartz was prominent in C14 and lithium diborate also became prominent at about 30% B_2O_3. It is probable that the exotherm peaks found for these glasses resulted from the nucleation and growth of lithium disilicate (fig. 6b).

4.2. Boric Oxide-Rich Compositions

4.2.1. DTA Results

DTA curves are given in fig. 8 for the D00 – D6 compositions lying approximately along the $Li_2O.2SiO_2$ – $Li_2O.2B_2O_3$ join. The series did not show a regular trend in exotherm peak temperatures and D0 gave two exotherms. This irregularity was also shown by the D11 – D16 series. High values were shown by D1 and D11 (30% SiO_2) and D4 and D14 (15% SiO_2); low values were shown by D2 and D12 (25% SiO_2), D5 and D15 (10% SiO_2), and D6 (5% SiO_2). A possible reason for this irregularity is discussed below.

The endotherms showed a more regular sequence (fig. 6a). Each composition showed two endotherms, a main endotherm which was below 800° C in the series D2 to D5, but above it in the series D11 to D16 and also in D6. A subsidiary peak appeared above 800° C in the first series, but below it in the second. The values lying above 800° C for D2 and D6, and D11

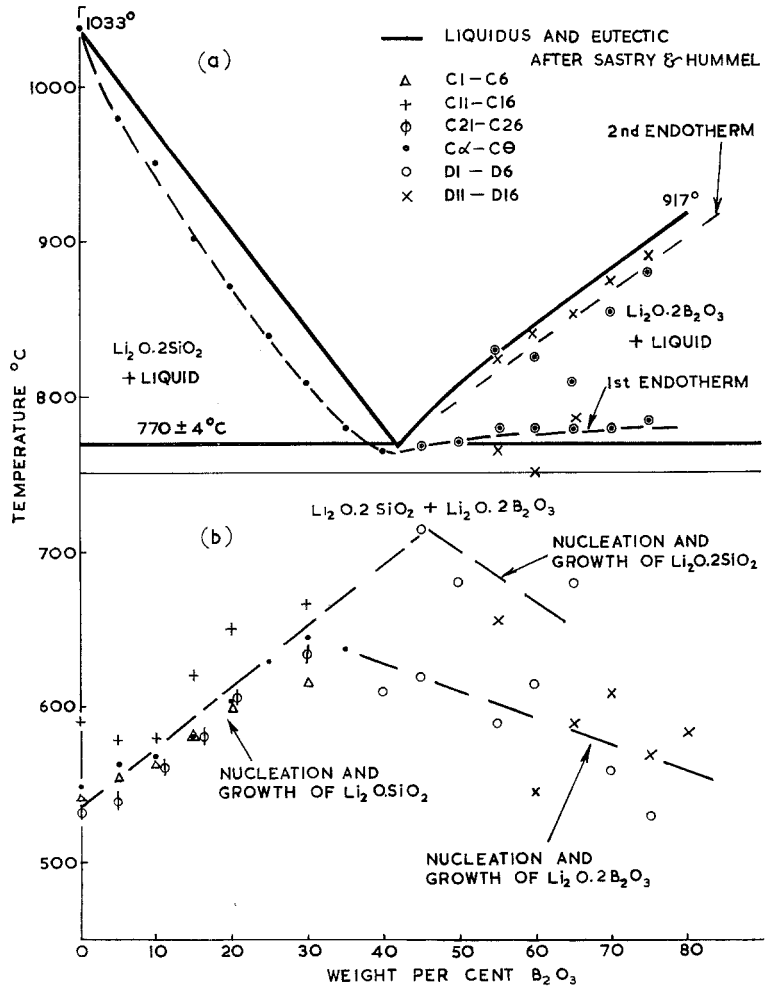

Figure 6 DTA peak temperatures of lithium borosilicate glasses versus boric oxide content. (a) Endotherms compared with liquidus values after Sastry and Hummel [3]; (b) Exotherms.

TABLE III DTA of silica-rich lithium borosilicate glasses. Areas under main exothermic peaks. (Arbitrary units)

B_2O_3 content Wt %	Sample	Area under peak	Sample	Area under peak	Sample	Area under peak	Sample	Area under peak
0	C 1	37	C 11	19	C 21	50	C α	40
5	C 2	26	C 12	25	C 22	37	C β	40
10	C 3	32	C 13	26	C 23	33		
						30	C γ	38
						32		
15	C 4	31	C 14	18	C 24	28		
						29	C δ	30
						35		
20	C 5	31	C 15	14	C 25	43	C ε	32
25	—	—	—	—	—	—	C ζ	32
30	C 6	27	C 16	6*	C 26	26	C η	28
35	—	—	—	—	—	—	C θ	24

*Doubtful value owing to base line shift.

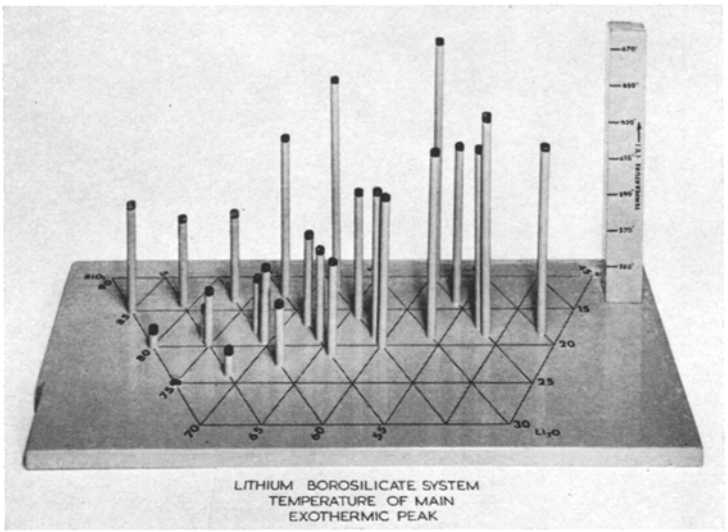

(a)

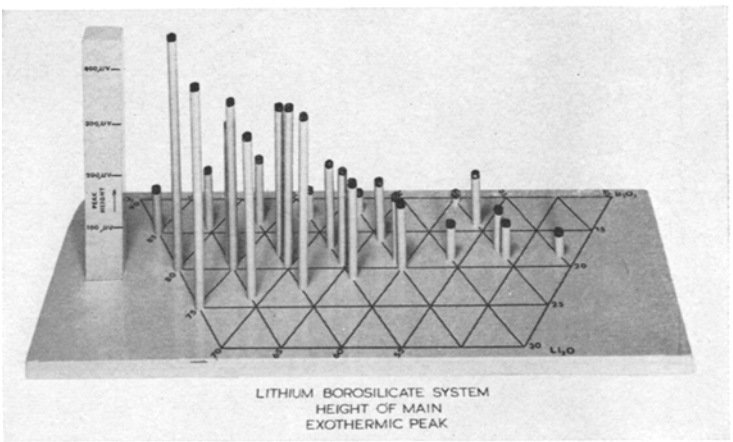

(b)

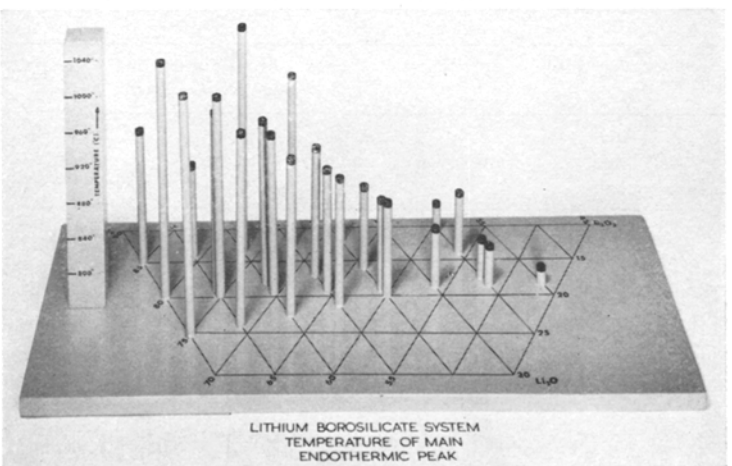

(c)

Figure 7 (a) Three-dimensional model of the exothermic peak temperatures and of compositions of the silica-rich glasses; (b) Three-dimensional model of the exothermic peak heights and of compositions of the silica-rich glasses; (c) Three-dimensional model of the endothermic peak temperatures and of compositions of the silica-rich glasses.

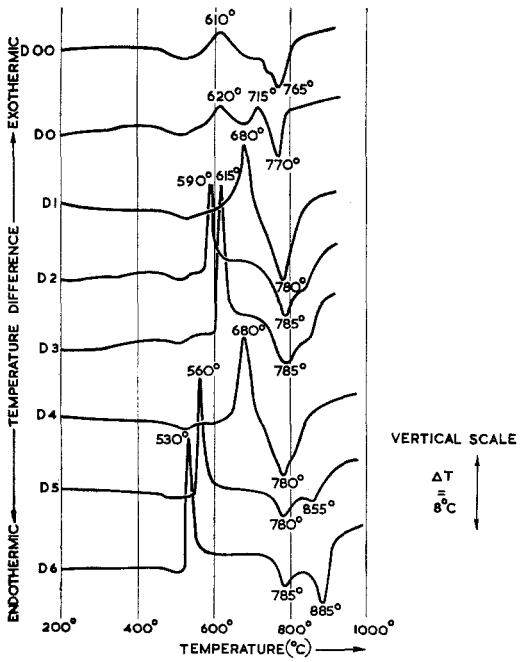

Figure 8 Differential thermal analysis of lithium borosilicate system. Boric oxide-rich compositions lying along the $Li_2O.2SiO_2$-$Li_2O.2B_2O_3$ join.

and D16 are in fair agreement with the liquidus values found by Sastry and Hummel [3]. The main endotherm for D00 and D0 at 770° C is in agreement with the eutectic value.

It is possible that the endotherms at ~ 780° C correspond to some local eutectic melting in the devitrified material.

4.2.2. X-ray Analysis of Sintered Products

Heat treatments were again carried out at temperatures below the eutectic at 770° C. Data on the crystalline products observed in the sintered material are given in table II.

The results obtained agree generally with the phase equilibrium relations given in fig. 1. Samples of composition lying near the eutectic consisted of a complex mixture of phases. The chief crystalline constituent of each sample was lithium diborate; lithium metasilicate, lithium disilicate and α-quartz were the secondary phases observed.

The compositions D11 and D12 were within the two-liquid field. With the more silica-rich compositions C11 to C16, D11 and D12 formed a continuous series with a progressive variation in nominal composition. The sequence C14 to D12 is of special interest as at least three crystalline phases are present in each of these samples. The phase constitution changed across the series; the major devitrification products were a mixture of lithium disilicate and α-quartz in C14, α-quartz in C16, and lithium diborate in D12, consistent with the phase equilibrium diagram by Sastry and Hummel [3].

The more highly sintered products, which have been denoted as grade 3 material (tables I and II), appear to be potentially useful as glass-ceramics. The texture of a typical example of grade 3 material, composition C6, is shown in the electron micrograph (fig. 9).

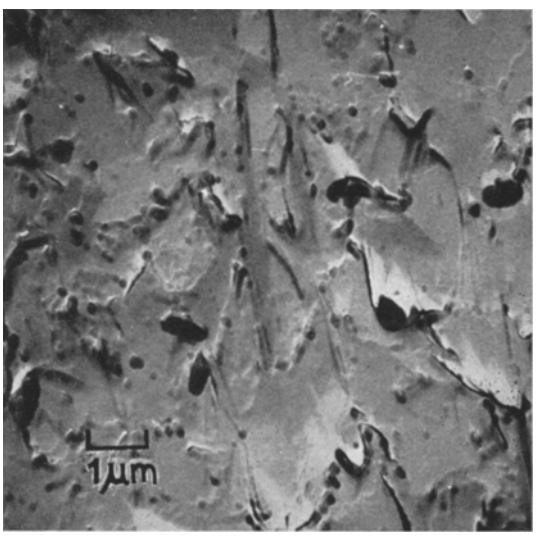

Figure 9 Electron micrograph of glass-ceramic composition. C 6, containing lithium disilicate, lithium diborate and some unidentified material. Two-stage replica Pt-C shadowed.

5. Summary and Conclusions

(*a*) The DTA endotherms obtained in this investigation showed regular changes in peak temperature in parallel with the compositional changes. They followed the same trends as the liquidus values reported by Sastry and Hummel [3] from equilibrium studies, but were generally somewhat lower than these. This discrepancy may be attributed to the presence of residual glassy phase in some of the devitrified glasses. However, the endotherm for the completely crystalline material obtained from $Li_2O.2SiO_2$ glass was 1037° compared with the published value of 1033° C for the mp of lithium disilicate.

(*b*) The boric oxide-rich compositions showed double endotherms. The lower peak in each case

may correspond to local eutectic melting between some $Li_2O.2SiO_2$ and $Li_2O.2B_2O_3$ crystals at $\sim 780°$ C. The second peak above 800° corresponded to the liquidus.

(*c*) The exotherms for the devitrification of the silica-rich glasses also showed regular trends corresponding to composition changes and generally the peak temperatures increased and peak strengths decreased with increasing B_2O_3 content. These peaks may be attributed to the nucleation and growth of lithium disilicate with boric oxide acting as a diluent.

(*d*) Although the exotherm(s) for a given boric oxide-rich glass sample was reproducible, the series investigated here did not show such regular trends with compositions as those found for the silica-rich series. Lithium diborate was present in all the devitrified compositions but some contained at least two of the following crystalline phases in significant amounts, namely, $Li_2O.2SiO_2$, $Li_2O.SiO_2$ and α-quartz.

(*e*) An exotherm above or below 650° C was shown by each composition but D0 containing 45% B_2O_3 and in the immediate vicinity of the eutectic, showed peaks at 620 and 715° C. It is probable that the exotherm peak temperature in each case was influenced by the first phase to nucleate and grow at an appreciable rate. For compositions with B_2O_3 content between ~ 40 and 65 wt% chance may have favoured one of two equally likely phases, lithium diborate or lithium disilicate (or even metasilicate). It is also possible that this primary phase was not the major phase found in the final sintered product.

In fig. 6b it is suggested that exotherms which occurred below 650° C for boric oxide-rich glasses were due to the primary nucleation and growth of $Li_2O.2B_2O_3$, and those above it were due to $Li_2O.2SiO_2$. In the case of D0 glass these two processes occurred to an equal extent.

(*f*) This investigation showed that glass compositions containing at least 25 wt% B_2O_3 could be sintered and devitrified at the respective exotherm peak temperatures to give hard, dense products similar in texture to glass-ceramics.

References

1. P. W. MCMILLAN, "Glass Ceramics" (Academic Press, 1964) p. 107.
2. B. S. R. SASTRY and F. A. HUMMEL, *J. Amer. Ceram. Soc.* **42** (1959) 81.
3. *Ibid* **43** (1960) 23.
4. F. W. WILBURN and C. V. THOMASSON, *J. Soc. Glass Tech.* **52** (1958) 158T.
5. Corning Glass Works, B.P.905, 253 (June 1960).
   C. G. BERGERON, C. K. RUSSELL and A. L. FRIEDBERG, *J. Amer. Ceram. Soc.* **46** (1963) 246.
   B. LOCARDI, *Vetro e Silicati* **9** (1963) 5.
   R. L. THAKUR, K. TAKIZAWA, T. SAKAINO and T. MORIYA, *Cent. Glass Ceram. Res. Bull.* **11** (1964) 1.
6. C. K. RUSSELL and C. G. BERGERON, *J. Amer. Ceram. Soc.* **48** (1965) 162.
7. L. F. OLDFIELD, *Compte rendu du symposium sur la fusion du verre, Brussels* (1958) 383 (published by Union Scientifique Continentale du Verre).
8. M. J. VOLD, *Anal. Chem.* **21** (1949) 683.
9. G. E. RINDONE, *J. Amer. Ceram. Soc.* **45** (1962) 7.